RSC Advances

PAPER

View Article Online
View Journal | View Issue

Cite this: *RSC Adv.*, 2020, **10**, 14892

Oleogelation using pulse protein-stabilized foams and their potential as a baking ingredient†

Athira Mohanan, Yan Ran Tang, Michael T. Nickerson and Supratim Ghosh *

Received 19th September 2019
Accepted 19th February 2020

DOI: 10.1039/c9ra07614j

rsc.li/rsc-advances

Structuring liquid oil into a self-standing semisolid material without *trans* and saturated fat has become a challenge for the food industry after the recent ban of *trans* fat by the US Food and Drug Administration and Health Canada. Lately, the use of hydrocolloids such as animal proteins and modified cellulose for oleogel preparation has gained more attention. However, plant proteins have never been explored for the development of oleogels. The present study explored the use of freeze-dried foams prepared using protein concentrates and isolates of pea and faba bean with xanthan gum at different pH values for oil adsorption and subsequent oleogelation. Compared to protein isolate stabilized foams, protein concentrate-stabilized foams displayed (i) higher oil binding capacity (OBC) due to a higher number of smaller pore size; and (ii) lower storage modulus and firmness due to the higher oil content. At all pH values, there was no significant difference between the OBC of different protein isolates, but among the concentrates, pea displayed higher OBC than faba bean at pH 5 and faba bean displayed higher OBC than pea at pH 9. Results showed that such oleogels could be used as a shortening alternative. Cakes prepared using the pea protein-based oleogel at pH 9 displayed a similar specific volume as that of shortening-based cake, although with higher hardness and chewiness.

1. Introduction

Structuring liquid oils into self-standing semisolid materials is essential for their use in baked products, such as cakes, pastries, muffins and cookies, where functionality, texture and palatability of the final product depend on the type of fat present.[1] Owing to the harmful effects of using *trans* fats in food, and their recent ban by the US Food and Drug Administration and Health Canada, food scientists are searching for alternative approaches to structuring liquid oils with tunable physicochemical properties. Oleogelators, such as plant waxes, fatty esters, mono and diglycerides, and ethyl cellulose, capable of converting a liquid oil into a self-standing semi-solid structure (known as an 'oleogel'), have widely been considered as a potential alternatives to *trans* and saturated fats.[1] Recently, the use of food hydrocolloids for the preparation of oleogels has gained more attention, and significant research effort is underway.[1–7]

Proteins are a widely used food-grade polymer with high nutritional value and have shown potential for use as oleogelators.[8,9] However, since proteins are insoluble in oil, a direct approach cannot be used to bind oil and induce gelation. Many indirect oleogelation approaches, such as the conversion of protein-stabilized emulsions,[5] foams,[7] and hydrogels[4,8,9] into oleogels, have been investigated. The foam-templated approach of oleogelation seems more feasible since there is no high-temperature drying as in the emulsion-templated approach or several steps of solvent exchange processes required for hydrogels to oleogel conversion. However, so far only hydroxyl propyl methylcellulose (HPMC)[7] and a combination of gelatin and xanthan gum (XG) have been used for foam-templated oleogelation.[2]

A number of plant-derived proteins are also available, which have the functional properties required for foam stabilization,[10] and hence have the potential for the oleogel preparation using the foam-templated approach. However, despite the growing consumer demand for plant-based protein sources, research on the use of plant proteins as oleogelators is non-existent. Therefore, the aim of this study was to examine the suitability of foams stabilized by different pulse proteins (*e.g.*, pea and faba bean protein concentrates and isolates) combined with xanthan gum for the oleogelation of canola oil (CO) and to evaluate their functionality as shortening alternatives. To our knowledge, pulse proteins have never been used for oleogelation. We recently showed that two pulse proteins from pea and faba bean along with xanthan gum at a range of pH values could be successfully used for foam generation.[11] Here we investigated how protein–polysaccharide interactions in the freeze-dried foam affect oil binding capacity, rheological and structural properties of the oleogels. The most suitable pulse protein foam-based oleogel was also tested in cake baking and

Department of Food and Bioproduct Sciences, University of Saskatchewan, 51 Campus Drive, Saskatoon, SK, Canada, S7N5A8. E-mail: supratim.ghosh@usask.ca; Tel: +1 306 966 2555

† Electronic supplementary information (ESI) available. See DOI: 10.1039/c9ra07614j

compared with cakes baked with CO and conventional highly saturated shortening.

2. Materials and methods

2.1. Materials

Pea protein concentrate (PPC; 47.9% protein, wet basis (w.b.); 6.1% moisture, 4.9% ash, 38.8% carbohydrate, and 2.2% lipid) was kindly donated by Parrheim Foods (Saskatoon, SK, Canada). Faba bean protein concentrate (FPC; 58.9% protein, wet basis (w.b.), 6.2% moisture, 5.9% ash, 26.6% carbohydrate, and 2.4% lipid) and isolate (FPI; 83.0% protein w.b., 5.9% moisture, 3.4% ash, 3.8% carbohydrate, and 3.9% lipid) were kindly donated by AGT Food and Ingredients (Saskatoon, SK, Canada). Pea protein isolate (PPI; 78.2% protein, w.b., 6.0% moisture, 6.0% ash, 8.2% carbohydrate and 3.6% lipid) was kindly donated by Nutri-Pea Limited (Portage la Prairie, MB, Canada); while xanthan gum (XG 83.7% carbohydrate, 9.4% moisture, 6.9% ash) was purchased from Bulk Barn Store (supplied by Duinkerken Foods Inc., Summerside, PEI, Canada). CO (Great Value brand) and 100% vegetable shortening (Crisco brand, composed of soybean oil, hydrogenated palm oil, modified palm oil, mono and diglycerides, TBHQ and citric acid) were purchased from Walmart Canada grocery store. Milli-Q™ water (Millipore Corporation, MA, USA) was used for all the solution preparation. All other chemicals were purchased from Sigma Aldrich, Canada.

2.2. Preparation and properties of foams

2.2.1. Foam preparation. Foams were prepared according to the method developed by Mohanan *et al.*[11] Stock solutions of proteins and XG were prepared separately with 0.02 wt% sodium azide and left at room temperature. On the next day, the desired amount of protein and XG solutions were mixed on a magnetic stirrer (400 rpm) for at least 30 minutes to get a 400 mL mixture. The pH was set to the desired value using 1 M NaOH or 1 N HCl prior to foam preparation. To identify the most suitable concentration of protein, XG and whipping time, foams were prepared by whipping mixtures of different concentrations of protein powder (0, 2, 5 and 10 wt%) and XG (0, 0.125, 0.25, and 0.5 wt%) solutions at different pH values (3, 5, 7 and 9) for different times (5–40 minutes). Whipping was done using a KitchenAid Ultra Power Mixer (KitchenAid, Whirlpool Canada LP, Mississauga ON) with a 4.5 qt (4.3 L) stationary bowl and stainless-steel rotating beaters at speed 8 (380 rpm). Solutions with higher protein (10 wt%) and XG (0.5 wt%) concentrations were highly viscous, and it was hard to incorporate air bubbles, while the solutions with low protein and XG concentrations were unable to keep the foams stable. All concentrations of XG alone was also unable to stabilize foams at any pH values. Foams prepared by whipping a mixture of 5 wt% protein (PPI, PPC, FPI or FPC) and 0.25 wt% XG at different pH values (3, 5, 7 and 9) for 20 minutes displayed the most optimal stability and were selected for the current study. Freshly prepared foams were immediately transferred to aluminum tray (20 cm × 20 cm × 4 cm) and frozen at −30 °C for 24 h and dried for 72 h using a freeze-dryer (Labconco FreeZone 18 Liter Console Freeze Dryers, Labconco Corp, Kansas City, Missouri, USA).

2.2.2. Foam microstructure. The microstructure of the freeze-dried foams was obtained using a bright field microscope (Nikon Eclipse E400 microscope, Nikon Canada Inc., Mississauga, ON, Canada) connected with a Nikon DS-Fi1 camera using a 10× objective lens at room temperature (25 ± 2 °C). The freeze-dried foams were cut into small slices (~0.5 mm thick) using a sharp blade for microstructure analysis. The samples were firm enough to hold the structure while cutting. The images were analyzed and processed using NIS-Elements F3.0 software. The bubble size was calculated manually using a scale bar in the software. At least three images from each replicate were used for bubble size analysis. The number of bubbles used for the average size calculation varied from 45 (in the samples displaying a higher number of smaller bubbles as in FPC-XG foam at pH 9) to 9 (in case of samples displaying larger bubbles, as in FPI-XG foam at pH 9).

2.3. Preparation and properties of the oleogels

2.3.1. Oleogel preparation. Oleogels were prepared by adding oil into the freeze-dried foams. Approximately 0.5 to 1 g dry foam was placed into a 50 mL centrifuge tube, followed by dropwise addition of CO with gentle shaking of the tube to improve oil–foam interactions. The added oil was instantly absorbed by the foams until it was saturated. Oil addition stopped when the foams taken in the centrifuge tube was completely 'wet', and the foams were no longer absorbing any oil. At this time, the excess oil floated on the top of the oleogel was separated by inverting the centrifuge tube.

2.3.2. Oil binding capacity. The oil binding capacity (OBC) was determined using a method described by Pehlivanoğlu *et al.*[12] with slight modification. Briefly, the tubes with oleogels were centrifuged for 20 min at 309 × *g* using a benchtop centrifuge (IEC clinical centrifuge, Damon Corp, Needham HTS, MA, USA). The tubes were then inverted and placed on a metal wire-mesh placed on top of a beaker, where the released oil was collected for 1 h. The weight of the tube with oleogel before (W_a) and after removing the released oil (W_b) was noted. The oil remained in the oleogel after centrifugation (W_f) was calculated using the initial weight of the oil added to the oleogel (W_i) and the amount of oil lost ($W_a - W_b$) according to eqn (1):

$$W_f = W_i - (W_a - W_b) \quad (1)$$

The oil binding capacity (OBC), a measure of final oil content per unit foam weight, was calculated by dividing W_f with the dry foam weight used to hold the oil according to eqn (2):

$$\text{OBC} = \frac{W_f}{\text{dry foam weight}} \quad (2)$$

2.3.3. Rheology of the oleogels. The viscoelasticity of the oleogels was determined using an AR-G2 rheometer (TA Instruments, Montreal, QC, Canada) equipped with a 40 mm cross-hatched parallel plate geometry to eliminate any slippage

during measurements. Oleogels (after removal of excess oil *via* centrifugation) were gently loaded on the Peltier plate of the rheometer with a spatula. An oscillatory strain sweep from 0.01% to 100% was then performed at a constant frequency of 1 Hz at 25 °C. The storage (G') and loss modulus (G'') of the samples were recorded with TRIOS Software (TA Instruments, Montreal, QC, Canada). The viscoelasticity of the oleogels was also measured as a function of temperature using the same geometry and the same amount of sample, while the temperature of the oleogels was varied from 15 to 100 °C at a rate of 5 °C min^{-1} and the G' and G'' were measured at a constant strain and frequency of 0.05% and 1 Hz, respectively, within the linear viscoelastic region.

2.3.4. Spreadability. The spreadability of the oleogels was measured using a texture analyzer (TA-Plus texture analyzer, Texture Technologies Corp.) fitted with a conical spreadability test probe (TA-425 TTC spreadability RIG). Measurements were made in compression mode with a penetration depth of 65 mm, test speed of 3 mm s^{-1} and a post-test speed of 10.0 mm s^{-1}. Before spreadability measurement, a sample was placed into the female cone, pressed gently to avoid any incorporation of air using a plastic spatula. The cone was then fixed on the bottom platform of the texture analyzer, and the sample surface was levelled. The male cone was used to compress the sample between the two cones and returned to the initial position. From the obtained data of force *vs.* distance, the maximum positive and negative forces (firmness and cohesiveness, respectively) and the area under the curve were calculated.

2.3.5. Fourier transform infrared (FTIR) spectroscopy. To understand protein conformation change during oleogelation and hence to uncover the mechanism of foam–oil interaction during oleogel formation, the secondary structure of all protein powders, freeze-dried foams, and oleogels were determined using ATR-FTIR microscopy. The Renishaw Invia Reflex Raman Microscope (Renishaw, Gloucestershire, UK) fitted with an Illuminated IR II FTIR microscope (Smith's Detection, Danbury, CT) along with a 36× ATR objective lens have been used for FT-IR measurement within a wavenumber range 4000–650 cm^{-1} with 4 cm^{-1} resolution. A small quantity of each sample was loaded on a glass slide and placed it under the ATR lens of the microscope and the desired part of the sample was focused. Then an average of 400 spectra was collected for each measurement and each sample was replicated twice. In the case of both foam and oleogel, the focus was given to the bubble boundaries so that the information on protein secondary structure during interaction with air and oil can be obtained. In the case of powder, the sample was pressed to obtain a small pellet before analysis. The powder of protein–polysaccharide mixtures at pH 9 was prepared by adjusting the pH of the corresponding protein–XG mixture to pH 9 and then freeze-dried. The secondary structure of proteins was determined from the amide I band (1600–1700 cm^{-1}). The second derivative of the spectra was used to identify the signature peaks of different secondary structures as described by Kong and Yu.[13] The characteristic peaks used were between 1612–1641 and 1690–1698 cm^{-1} for beta-sheet; 1650–1658 cm^{-1} for alpha-helix; 1662–1688 cm^{-1} for beta-turn; and 1640–1645 cm^{-1} for random coil. Each secondary structure was quantified using the sum of the area under the corresponding peaks using Renishaw's WiRE 3.3 software.

2.4. Preparation and characterization of cakes

2.4.1. Cake baking with oleogel. Cakes were baked using the AACC International Method 10-90.01.[14] In brief, 200 g of all-purpose flour, 280 g of crystalline sugar, 100 g of fat, 24 g of non-fat dried milk, 18 g of dried egg white powder, 6 g of NaCl, 12.5 g of baking powder, and 250 g of water were used for the cake preparation as recommended by the AACC method.[14] The batters were made using a KitchenAid Ultra Power Mixer (KitchenAid, Whirlpool Canada LP, Mississauga ON) with a 4.5 qt (4.3 L) stationary bowl and rotating stirrers. For the fat phase of the batter, three different materials were used: vegetable shortening, CO and the oleogel (PPC-XG at pH 9). All the dry ingredients were mixed before adding them into the mixing bowl. Then the fat phase was added with 150 mL of water and mixed for 1 min at speed 2 followed by 4 min at speed 4. The rest of the water was added in steps with various mixing speeds according to the AACC method.[14] Approximately 200 grams of dough was then transferred to a baking tray (15.0 × 7.5 × 5.5 cm) and baked in an electric oven at 190 °C (375 °F) until done according to the AACC method.[14] After baking, the cakes were left in the baking tray for 30 min at room temperature, carefully removed from the tray, and covered with aluminum foil and plastic wrap to keep moisture until further analysis.

2.4.2. Characterization of cake batters and cakes. Confocal laser scanning micrographs of different cake batters were taken using a Nikon C2 microscope (Nikon Inc., Mississauga, ON, Canada) using a combination of 543 and 633 nm lasers, and 10× and 40× objective lens. Nile red (excitation by 543 nm laser, emission collected in 573–613 range) and fast green (excitation by 633 nm laser, emission collected with a 650 nm long-pass filter) were used to stain the oil phase and the proteins in the aqueous phase, respectively. For oleogel batters, 0.01 wt% Nile red was dissolved in liquid CO prior to its addition to the dry foam, while for shortening batter, 0.01 g of Nile red was dissolved 1 g CO and mixed with 100 g shortening. To stain the proteins, 3 drops of 0.1 wt% fast green solution in water was added to 150 mL of water used for batter preparation. Batters were analyzed within one hour after preparation. A small amount of batter was taken on a glass slide, compressed gently with a cover slide and used for image capturing.

The viscosity and viscoelasticity of cake batters were measured using the AR-G2 rheometer (TA Instruments, Montreal, QC, Canada) with a 40 mm acrylic parallel plate. Viscosity analysis was carried out by rotational shear mode at 25 °C with a gap of 500 μm and as a function of increasing shear rate from 0.01 to 1000 s^{-1}. For viscoelasticity, oscillatory strain sweep (from 0.01% to 100%) was applied at a constant frequency of 1 Hz at 25 °C to find out the linear viscoelastic region, and then a frequency sweep measurement was performed from 0.01 to 10 Hz at a constant strain of 0.05%.

The specific gravity of the cake batters was determined from the ratio of the weight of a certain volume of batter to the weight

of the same volume of water. The specific volume of the cakes was obtained using the ratio of the volume of cake, to the weight of the cake. The cake volume was determined using rapeseed displacement procedure according to AACC 10-05 method.[15]

Texture profile analysis of prepared cakes was measured using a texture analyzer (TA-Plus texture analyzer, Stable Micro Systems Ltd. Surrey, UK), 24 h after baking according to Kim *et al.*[16] with slight modification. Pieces of cake samples were cut into 2 cm cubes and compressed two times with a cylindrical probe of diameter 2.5 cm at a speed of 2 mm s^{-1} until the height of the cake pieces were 50%. The hardness, springiness, cohesiveness, gumminess, and chewiness were measured from the texture profile analysis using the Exponent software (version 6.1.4.0, Stable Micro Systems Ltd.) according to Friedman *et al.*[17]

2.5. Statistical analysis

All foams and oleogels were prepared in triplicates. Three batches of cakes were prepared for each formulation. All the other experimental measurements were carried out in triplicate using different foam, oleogel and cake samples, and the average and standard deviation are reported in the manuscript. The results were statistically analyzed from the analysis of variance and *t*-test at a significance level of 5% using Microsoft Excel 2013.

3. Results and discussions

3.1. Development of pulse protein-stabilized foams

Foams were freeze-dried to obtain a porous structure essential for oil absorption. Freeze drying resulted in the formation of a self-standing porous sponge-like structure, except for the foams prepared at pH 3, which destabilized during freeze-drying, and appeared as a powder. Therefore, the foams prepared at pH 3 were excluded from oleogel preparation. The ability of any porous structure to adsorb oil is related to their microscopic pore size, pore density, connectivity between the pores and the interaction between the oil and the material used for the preparation of porous structure.[18,19] Therefore, the microstructure of the freeze-dried foams was determined and their average pore (bubble) size was calculated from the corresponding microscopic images (Fig. 1). In general, the protein concentrate foams (Fig. 1b and d) displayed smaller pore sizes, and a homogeneous distribution of pores at all pH values compared to the corresponding protein isolate-stabilized foams (Fig. 1a and c). For example, the average pore size of PPC and FPC foams was 227.4 ± 78.7 μm and 193.6 ± 45.4 μm at pH 9 compared to the pore size of 741.1 ± 210.8 μm and 1197.9 ± 224.1 μm for PPI and FPI foams, respectively. PPC and FPC foams displayed thick boundaries around the pores at both pH 7 and pH 9 compared to pH 5, such that a clear separation between the bubbles could be observed in the majority of the foam microstructure (Fig. 1b and d). For PPI and FPI foams at pH 5, no clear boundaries between the pores were observed, most of the pores were broken, and some powders of freeze-dried protein–XG mixtures were also observed (Fig. 1a and c). A stronger dry-foam structure at pH 7 and 9 compared to pH 5 could be due to a thicker and stronger viscoelastic interface formed at the higher pH values. Also, the ability of protein concentrates to provide a stronger dry foam structure compared to the isolates could be due to the presence of additional polysaccharides in the concentrates which could provide additional stability to the air bubbles by forming a viscous and thick barrier around them.[20] Moreover, the higher lipid content present in the protein isolates might have also negatively affected the adsorption of proteins on the air–water boundaries and decreased the strength of the protein foam network. It is known that the foamability of proteins are influenced by the presence of lipid. For example, the foaming properties of egg white proteins were negatively affected by the addition of fat.[21]

3.2. Oleogelation

Oleogels were prepared by adding CO to the freeze-dried porous foams. Dry foams readily adsorbed liquid CO and facilitated the formation of soft self-standing gel-like structures, as seen in Fig. 2a. The protein foam network holding the oil was clearly visible under polarized light as dark rings (Fig. 2b). The affinity of these porous structures to the oil might be due to the interaction of oil with the hydrophobic patches on the proteins at the pore surface, similar to the mechanism of oil binding of HPMC foam described by Patel *et al.*[7] It is known that to accommodate the hydrophobic phase (such as air and oil), proteins must open up their structure to expose the internal hydrophobic patches.[22,23] In the present case, hydrophobic patches exposed during foam formation remained at the air bubble interface after the freeze-drying and interacted with the oil at the pore surface.

3.2.1. Oil binding capacity of the oleogels. Oil binding capacity (OBC, final oil content bound to the matrix per unit weight of foam) of the oleogels is displayed in Fig. 2c and d. Higher final oil content (OBC) indicates the greater ability of the freeze-dried foam to bind and retain oil. Overall, porous structures obtained from foams made of protein concentrates displayed higher OBC at all pH values than those prepared with isolates. For example, OBC of PPC and FPC foams at pH 9 was 25.1 ± 0.5 and 27.8 ± 1.2, respectively, which were significantly higher than the OBC of foams stabilized by corresponding protein isolates (17.2 ± 3.9 and 14.4 ± 1.6 for PPI and FPI, respectively at pH 9). Freeze-dried foams stabilized by all proteins at pH 5 displayed the least OBC compared to all other foams stabilized at other pH values. Highest OBC was obtained at pH 9 in the case of protein concentrates and pH 7 in the case of protein isolates. It should be noted that the highest OBC of protein stabilized foams in the present study was significantly lower than that of oil holding capacity of 98.8 g g^{-1} of dry foams obtained using 1 wt% hydroxypropyl methylcellulose (HPMC).[7] Such higher OBC could be due the reporting of loosely adsorbed oil (no centrifugation was used), and not the actual amount of oil bound to the system. The OBC of pulse protein–XG stabilized foams were also lower than that of gelatin–XG stabilized foams, which was able to adsorb 40–50 times oil per unit foam weight, equal to about 90% binding of adsorbed oil.[2] In the present

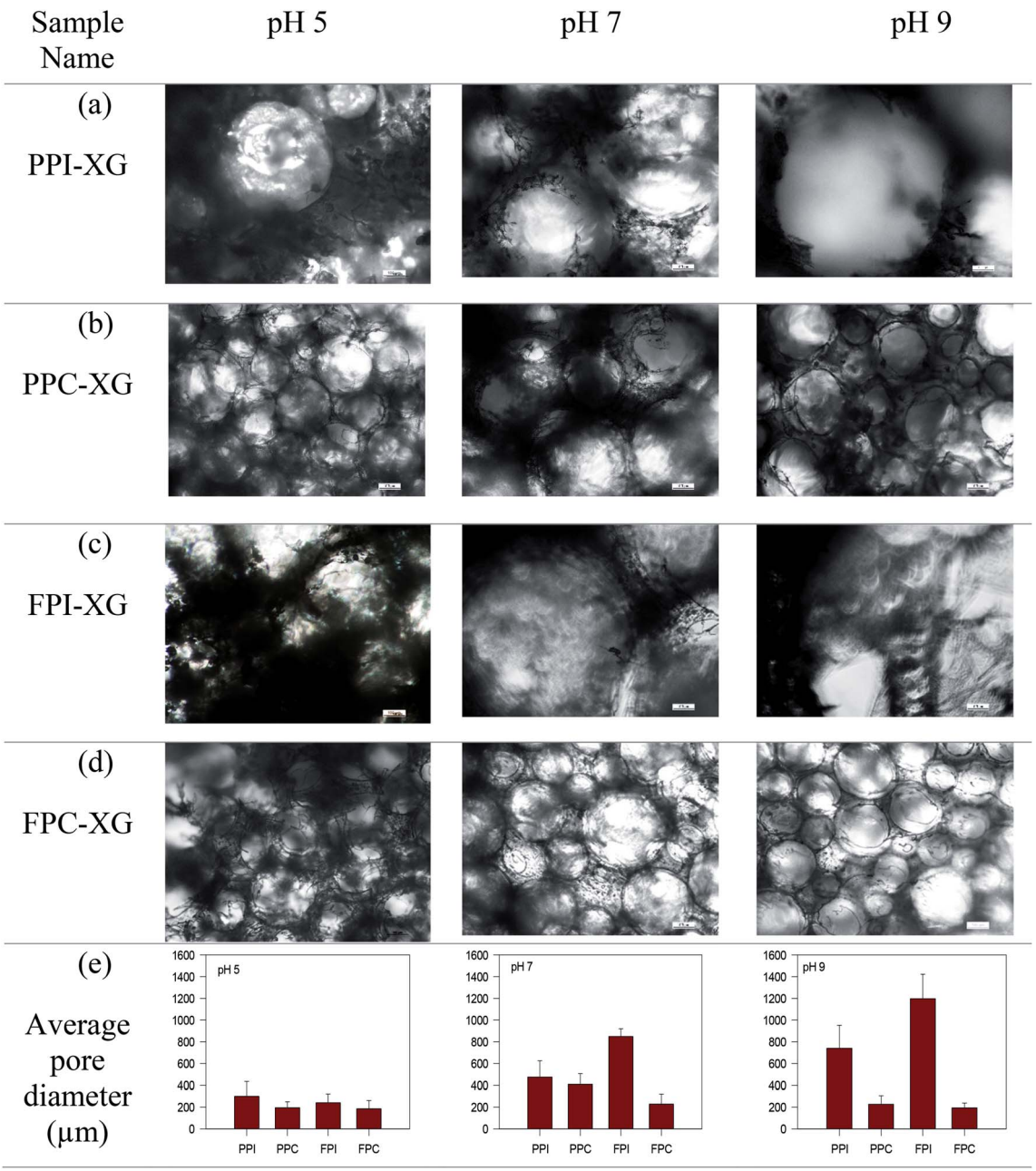

Fig. 1 (a–d) Microstructures of different freeze-dried foams stabilized by protein–xanthan gum mixtures prepared at different pH values, taken by light microscope using a 10× objective lens at room temperature. (e) Average bubble size of different freeze-dried foams prepared at different pH values measured from the micrographs (a–d). The black circles observed in the microscopic images of foams represents the bubble boundaries and the pores of the freeze-dried foams were located inside these boundaries.

case, the pulse protein–XG foams were able to retain only 70–80% of the adsorbed oil.

Higher OBC for protein concentrate-stabilized foams compared to protein isolates could be due to the smaller pore size and a higher number of pores in the former (Fig. 1). Since the hydrophobic patches on the proteins may cover a large surface area when the pores are smaller, protein concentrate-foams could effectively bind a larger amount of oil compared to protein isolate-foams. Also, as discussed before, the presence of a significantly higher amount of polysaccharide in the concentrates compared to the isolates could provide additional stability to the freeze-dried foam against oil loss during centrifugation, leading to a higher OBC. Although the pore sizes in PPC and FPC foams at pH 5 were similar ($p > 0.05$) as that of pH 7 and pH 9 (Fig. 1e), the foams prepared at pH 5 were weaker (Fig. 1) and they shrank and collapsed during oil addition, indicating a poor foam strength, which resulted in significantly lower OBC at pH 5 compared to pH 7 and 9. Therefore, not only the microscopic pore size but also the strength of the protein network was responsible for the OBC of freeze-dried protein

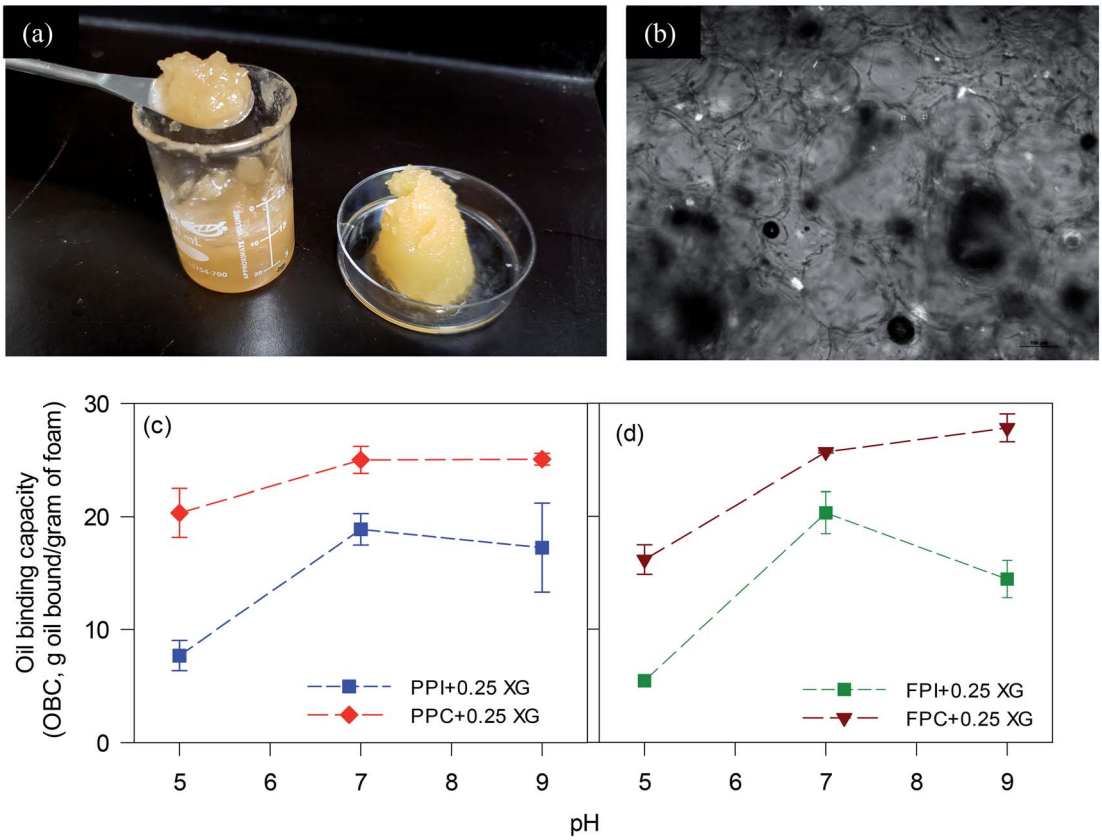

Fig. 2 (a) Appearance of protein foam-templated oleogel and (b) its polarized light microstructure. Oil binding capacities (OBC) of (c) PPI, PPC and (d) FPI and FPC foams prepared at different pH values are also shown.

foams. It should be noted that the strength of the protein network discussed here is qualitatively based on their microstructure and behaviour during oil addition as quantitative determination of protein network strength of foam or freeze-dried foam was not possible. Our previous work on foam stability revealed no significant difference between these pH values,[11] and interfacial rheology of quiescent protein film would not represent the appropriate interface of foam bubbles.[24]

3.2.2. Mechanism of protein–oil interaction during oleogelation. It has been reported that the secondary structure of protein changes while they adsorb on hydrophobic surfaces such as oil and air during emulsion and foam formation.[25,26] To investigate the effects of foam and oleogel formation on the protein's secondary structure, FTIR spectra of protein–XG powder, freeze-dried foams and oleogels were collected.[13] Because the oleogels from pH 9 foams were most stable and had higher OBC, only the pH 9 samples were used for FTIR analysis. To understand the effect of pH, the FTIR spectra of one of the oleogel (FPC-XG) was also collected at pH 5, 7 and 9 (Fig. S1, ESI†). FTIR spectra of the oleogels displayed peaks of both freeze-dried protein foams and canola oil (Fig. S1a†). There were no new peaks detected in the oleogels, but some of the peaks displayed a shift towards either lower or higher wavenumber (Table S1†), indicating some interaction between oil and protein. Major peaks of oleogels were between 1109–1155 cm^{-1} (C–O stretching), 1236–1240 cm^{-1} (C–O), 1453–1459 cm^{-1} (C–N), 1529–1534 cm^{-1} (–NH), 1642–1644 cm^{-1} (stretching vibrations of the C=O), 1744 cm^{-1} (C=O, originated from CO), 2852–2874 cm^{-1} (symmetric CH_2 stretching), 2924–2925 cm^{-1} (antisymmetric CH_2 stretching) and 3280–3295 cm^{-1} (hydroxyl groups (–OH) of polymers in the freeze-dried foams), which was similar to the FTIR spectra of oleogels prepared using gelatin–XG stabilized foam[2] and other biopolymer-stabilized oleogels.[27,30] In the present case, the shift of peak positions of symmetric and antisymmetric stretching vibrations of C–H bonds of canola oil towards higher wavenumber (2921 in canola oil to 2924–2925 in oleogel, and 2852 in canola oil to 2854–2875 in oleogel) was observed (Table S1†), indicating the change in chemical environment of protein and oil due to their interaction. Moreover, shift in peaks around 3280–3285 cm^{-1} in foams towards higher wavenumbers in oleogels (around 3290–3295 cm^{-1}), and shifts in amide II band positions indicate decrease in hydrogen bonding between protein–XG or intramolecular hydrogen bonding present in protein and concomitant increase in hydrophobic interaction between the protein and oil during oleogel formation.[28,29] Therefore the protein–protein and protein–XG network formed *via* hydrogen bonding is altered by the addition of liquid oil during the formation of oleogels. Stretching of –OH bands were mostly influenced by the change in pH of the foams used for oleogel preparation, which indicates that the intermolecular and the intramolecular

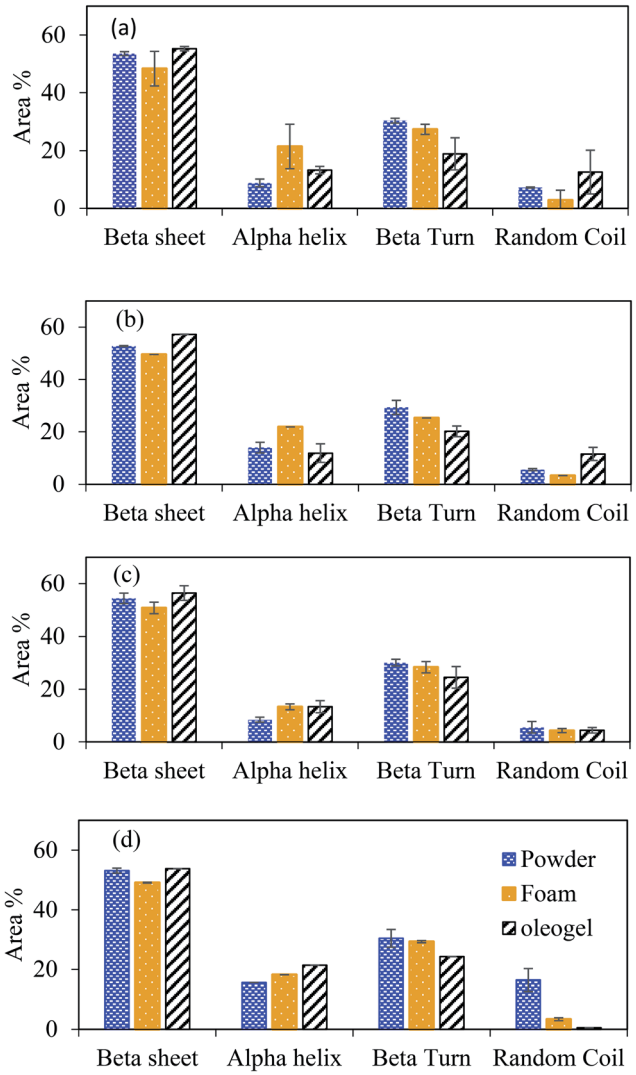

Fig. 3 The area% of characteristics secondary structure peaks of (a) PPI-XG, (b) PPC-XG, (c) FPI-XG and (d) FPC-XG powder, freeze-dried foam and corresponding oleogels at pH 9.

hydrogen bonding in the oleogels were mostly influenced by pH of the foams used for oleogel preparation.

Smoothed second derivatives amide I band of FTIR spectra for each protein powder, foams and their oleogels are provided in Fig. S2 (ESI†). Examples of second derivatives amide I band and their corresponding de-convoluted peaks for FPC-XG mixed powder, foam and oleogel are also shown in Fig. S3 (ESI†). Each secondary structure component was quantified by their peak area percentage and is shown in Fig. 3. The changes in percent peak areas of protein concentrates and isolates displayed similar trends in the secondary structure during foam and oleogel formation. In general, beta-sheet reduced in all protein–XG mixtures during foam formation, while it increased when the foam transformed into the oleogel. Alpha helix increased in all foams, but it decreased when the foam was transformed into the oleogel for PPI and PPC (Fig. 3a and b). For FPI (Fig. 3c) insignificant change in alpha-helix content was observed when the foam was transformed into the oleogel, while for FPC, it was increased (Fig. 3d). The content of beta-turn decreased for all when powder protein samples transformed into foams and oleogels. Random coil content decreased during the transformation of powder into foam and increased when the foam was transformed into the oleogel for both the pea proteins (Fig. 3a and b), while for both the faba bean proteins it decreased during both the foam and oleogel formation (Fig. 3c and d).

Analysis of protein secondary structure indicates that beta turns are unfavourable to accommodate hydrophobic oil into the protein network; hence their content decreased significantly when the protein foams were converted into oleogel. However, the suitability of the random coil structure towards oil depends on the protein type. It was reported previously that the proteins adsorbed on a hydrophobic surface take random coil structure at the early stage of adsorption, and at a later stage, convert into an alpha helix and beta-sheet conformation.[25] In the present case, an increase in the beta-sheet structure was seen for all proteins upon oil adsorption, indicating more hydrophobic interactions. For alpha helix, an increase was observed for the faba bean proteins at the expense of random coil; however, for both the pea proteins, alpha helix decreased while the random coils remained higher. Therefore, the changes in alpha-helix and random coil structures in different oleogels depended on the protein type and the presence of non-protein materials.

Overall, the FTIR analysis showed that during the formation of oleogels, hydrogen bonding between the biopolymers decreased while hydrophobic interaction increased. Similar changes in intermolecular interactions were also observed in gelatin–XG foam stabilized oleogels.[2] Also, an increase in oil loading was reported in the case of whey protein aerogel with increased hydrophobic interaction.[30] All of these reveals that the hydrophobic interaction might be the major interaction in the formation of protein-stabilized oleogels. Both van der Waals and hydrophobic interactions reduce when the distance between the two objects increases. Therefore, when the pores were large in size, the interaction between the protein foam surface and the oil in the middle of the pore would be weak, leading to a lower OBC for the foams with a larger pore size (Fig. 1 and 2).

3.2.3. Viscoelasticity of the oleogels. Changes in G' and G'' of the oleogels as a function of oscillatory strain are shown in Fig. S4 (ESI†). A typical behavior shown by all the oleogels is a brief linear region of G' at lower strains which decreased and dropped at a critical strain (yield strain). With an increase in strain, G'' increased to a maximum and started decreasing after crossing over G'. All the oleogels displayed higher G' than G'' before the crossover strain, indicating the formation of a gel-like structure. The linear viscoelastic region of the oleogels was short indicating gel formation occurred *via* weak interaction between the proteins and the oil.[7] The nature of the viscoelastic behaviour of protein foam-templated oleogels is also similar to that of the modified cellulose foam-templated oleogels reported in the literature.[7]

To directly compare, G' at 0.05% strain and crossover strain of all oleogels were re-plotted in Fig. 4. The strain 0.05% fell within the linear viscoelastic region of the oleogels; therefore,

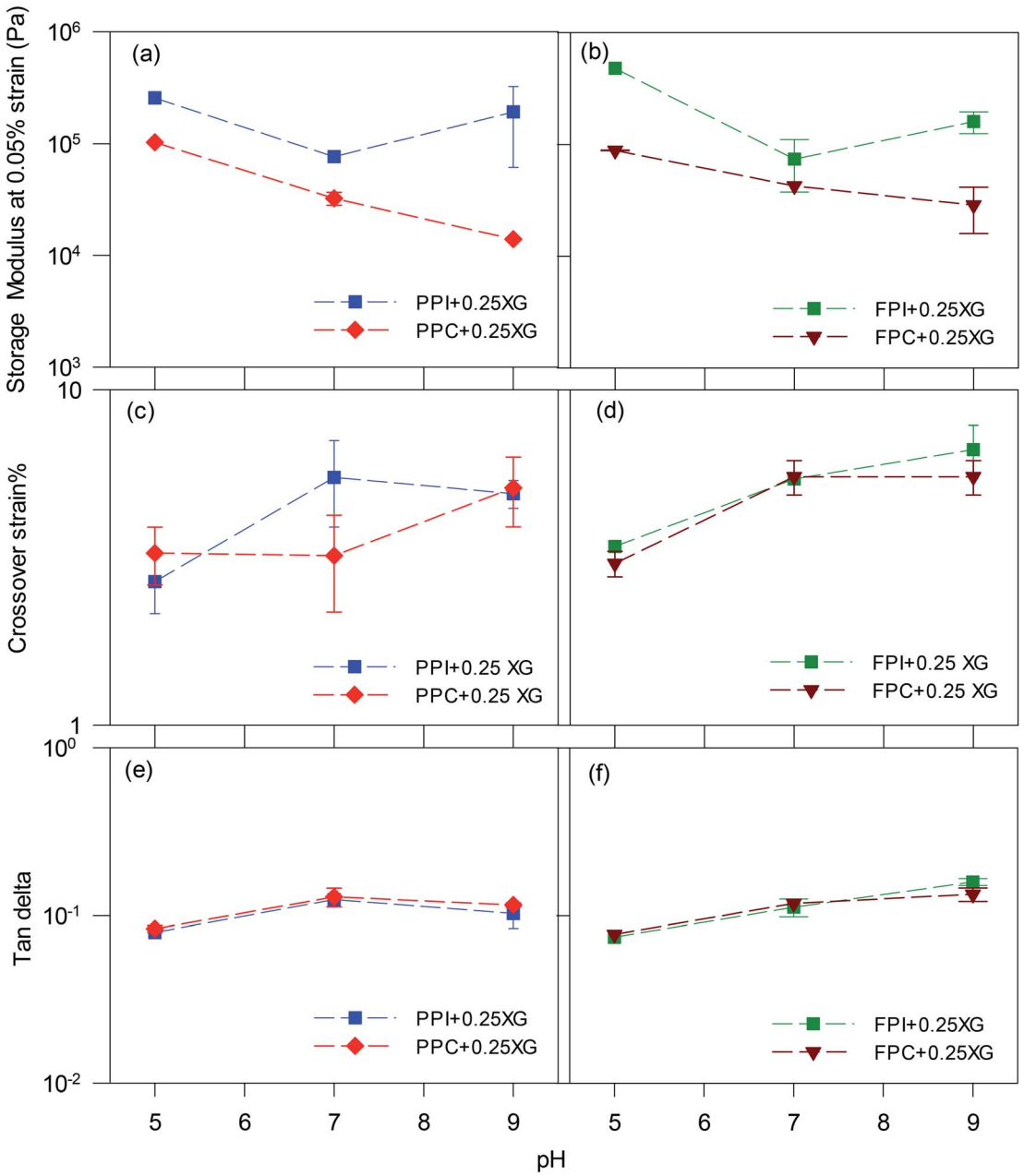

Fig. 4 The (a and b) storage modulus at 0.05% strain, (c and d) cross-over strain, and (e and f) tan delta at 0.05% strain of various oleogels prepared using (a, c and e) PPI-XG and PPC-XG, and (b, d and f) FPI-XG and FPC-XG at different pH values.

the G' values would be representative of an un-disturbed gel structure. Oleogels prepared with protein isolates displayed higher G' than the corresponding protein concentrate-stabilized oleogels at all pH values ($p < 0.05$) (Fig. 4a and b), which could be due to the lower oil content of the protein isolate-stabilized oleogels (Fig. 2c and d). Also, the protein isolate-oleogels had a higher quantity of protein which might have exerted higher resistance against oscillatory strain, thereby increasing the gel strength. Irrespective of protein type, all oleogels made with pH 5 foams displayed the highest gel strength but least crossover strain (Fig. 4c and d), indicating a brittle foam network which could be broken at a lower strain. Crossover strain increased with an increase in pH, indicating more force will be required to break the gel network at higher pH values. The tan delta values (Fig. 4e and f) remain around 0.1 for all oleogels at any pH value indicating elastic gel-like structure within the LVR.

The effect of temperature on the viscoelastic behaviour of oleogels was also investigated at a constant strain and frequency within the linear viscoelastic region. Results for only PPC and FPC oleogels at pH 9 are shown in Fig. 5, since they had higher oil content, and could be used in the baking application. The G' values of both the oleogels were significantly higher than the G'' values in the temperature range studied. Initially, very little change in G' was observed up to 80 °C, then it started decreasing

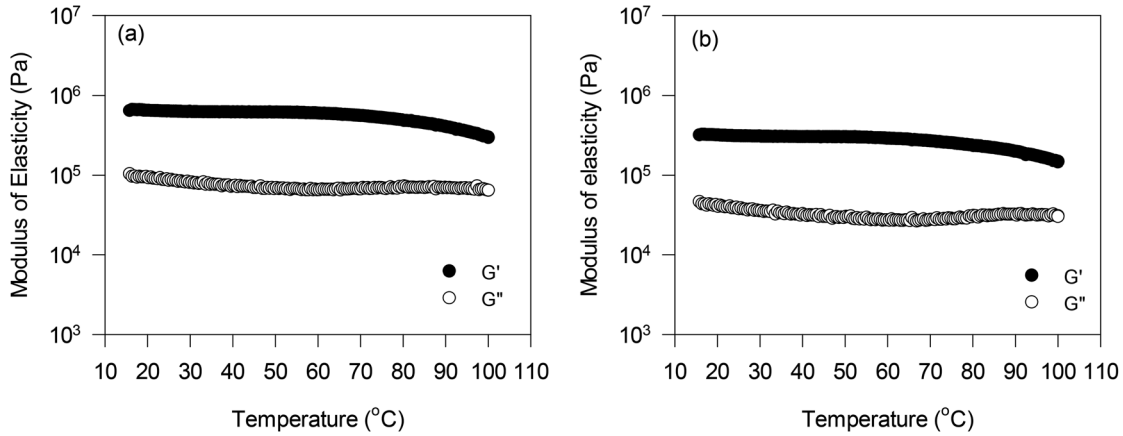

Fig. 5 Effect of temperature on viscoelasticity of oleogels prepared using foams stabilized with (a) PPC and (b) FPC at pH 9. Data collected at a constant strain of 0.05% and a constant frequency of 1 Hz. Temperature was raised at 5 °C min^{-1}.

with further increase in temperature. This could be due to some structural breakdown due to the decrease in hydrogen bonding within the protein network at a higher temperature, which led to an increase in the flowability of the oleogels. Patel *et al.*[7] also reported a similar decrease in both G' and G'' values of HPMC foam-stabilized oleogels with an increase in temperature. It should be noted that the PPC and FPC oleogels displayed higher G' and G'' values than the HPMC oleogels,[7] which were in the order of 10^4 Pa.

3.2.4. Spreadability of the oleogels. The spreadability of oleogels gives an indication of its firmness and the ease of handling during further food processing. Based on the texture analysis, a lower firmness means the oleogel would be more easily spreadable. The spreadability of a highly saturated vegetable shortening was also determined as a control. Oleogels made from protein concentrates displayed significantly lower firmness (higher spreadability) than the corresponding protein isolate-stabilized oleogels at all pH values ($p < 0.05$) (Fig. 6a and b). For example, the firmness of the oleogel made of PPC at pH 7 (37.6 ± 2.1 N) and at pH 9 (37.2 ± 5.4 N) was almost half of the firmness of the PPI-oleogels. The firmness of protein concentrate stabilized oleogels were also lower than that of a commercial shortening indicating it would be easier to spread these oleogels than the shortening (firmness of shortening was 46.5 ± 1.03 N, shown by a dashed line on Fig. 6). Similar to G', the firmness of the oleogels was also determined by the final oil content and the microstructure of the foams. Oleogels displayed higher firmness (lower spreadability) when the oil content was low, as in FPI and PPI oleogels. The protein isolate-stabilized oleogels were very much like a rigid sponge with only about 20% oil. When this oil became separated from the gels during compression, the rest of the material was hard to compress giving rise to higher firmness. Oleogels stabilized by protein concentrates at pH 9 had significantly higher oil content (more than 40% oil), which formed a consistent gel and the oil remained in the foam network during compression leading to

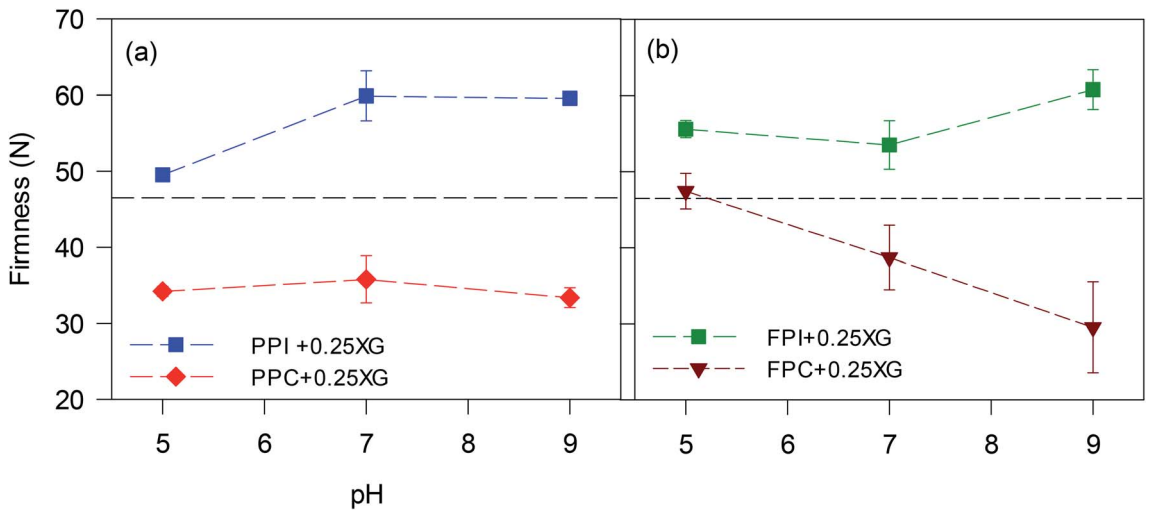

Fig. 6 Results of spreadability test expressed as firmness of oleogels made with (a) PPI and PPC, and (b) FPI and FPC. Spreadability of a commercial shortening is shown on the graph with a dashed line.

Table 1 Specific gravity of cake batters and specific volume of cakes baked using shortening, canola oil and oleogel. Different letters in each column indicate statistically significant difference ($p < 0.05$)

Sample	Batter specific gravity	Cake specific volume (mL g^{-1})
Shortening	0.87 ± 0.06^{a}	2.21 ± 0.05^{a}
Canola oil	1.23 ± 0.03^{c}	2.14 ± 0.16^{a}
Oleogel	1.15 ± 0.01^{b}	2.33 ± 0.05^{a}

a lower firmness (more spreadable) than the corresponding protein isolate stabilized oleogels. Reduction in firmness with an increase in oil content of the oleogels was also observed by other researchers.[4]

Overall, the microstructures of the foams, as well as the affinity of foams to bind the oil, played crucial roles in determining the viscoelasticity and spreadability of oleogels. PPI and FPI oleogels, with lower oil content and higher firmness, were not suitable for replacing shortening. Protein concentrate foams at pH 9, with smaller pore size, stronger protein network for pore stability displayed higher ability to bind oil and made consistent oleogel, which were easy to spread and could be suitable for shortening replacement in a baking application.

3.3. Cake baking with oleogel

The role of shortening (rich in saturated fat) in cake is to increase air incorporation, cover the gluten and starch particles present in the flour, reduce the gluten network, and increase the lubrication and moisture retention.[31] Shortening helps produce a softer final product with a delicate flavour. To see the effectiveness of oleogel as a shortening alternative, cakes were prepared by entirely replacing shortening with an oleogel prepared from PPC-stabilized freeze-dried foam at pH 9. The oleogel prepared from this particular foam was chosen since it provided a stable oleogel with high oil binding capacity (Fig. 2a) and a firmness closest to the shortening (Fig. 6a). This particular oleogel had more than 95% liquid CO (OBC of 25.05 g oil/g dry PPC foam is equivalent to 95.6% oil content). Cakes were also baked using 100% CO for comparison.

3.3.1. Properties of the cake batter. The cake batters prepared using shortening displayed the least specific gravity, followed by the oleogel and CO (Table 1), indicating higher air incorporation in the presence of shortening. The fat crystals present in the shortening might have stabilized the air bubbles incorporated in the batter during mixing, thereby lowering the better specific gravity.[31] Liquid oil is unable to stabilize the air bubbles by itself and also prevents proteins from stabilizing air bubbles in a continuous medium, leading to an increase in specific gravity for CO batter.[31] Oleogel batter displayed slightly lower specific gravity than CO batter ($p < 0.05$). A confirmation of air incorporation in the batter can also be seen from their microstructure (Fig. 7). In the shortening batter (Fig. 7a and d), protein (stained with green) and carbohydrate-rich phase are dispersed in the continuous fat phase (stained with red). The fat phase is filled with numerous air bubbles (appeared dark) which are supposedly stabilized by the fat crystals formed by the saturated fatty acids of shortening.[32] The most significant difference in the microstructure of CO (Fig. 7b and e) and

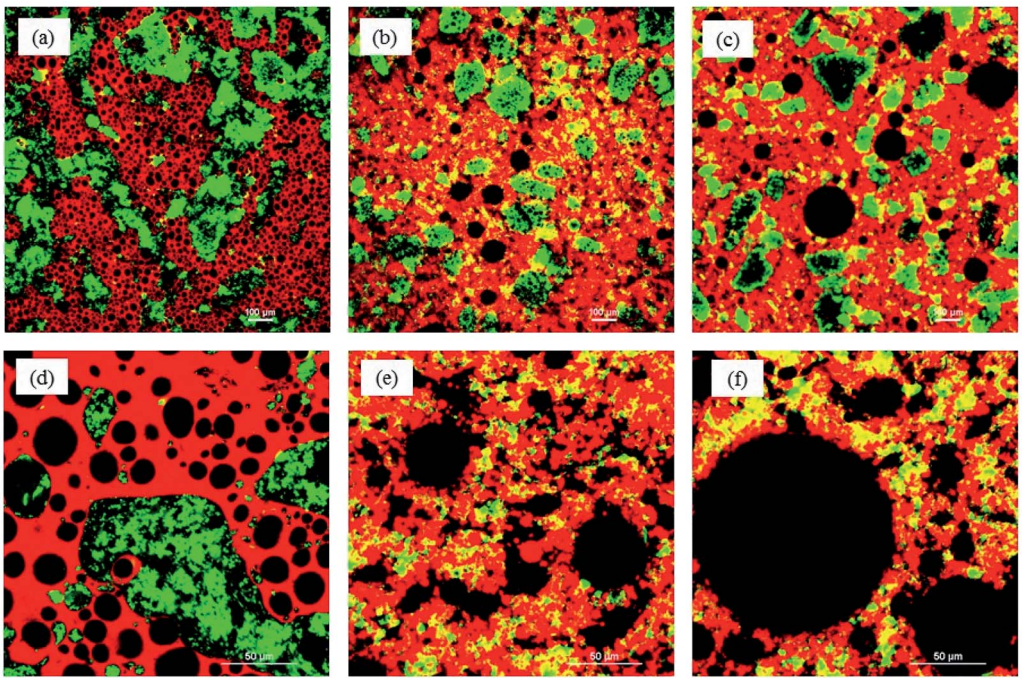

Fig. 7 Confocal micrographs of cake batters prepared with (a and d) shortening, (b and e) canola oil and (c and f) PPC oleogel (pH 9) using (a–c) 10× and (d–f) 40× magnification lenses. Green color (fast green) represents proteins, red color (Nile red) represents oil phase, and the starch and air bubbles are in black. The yellow color is the combination of red (oil) and green (protein).

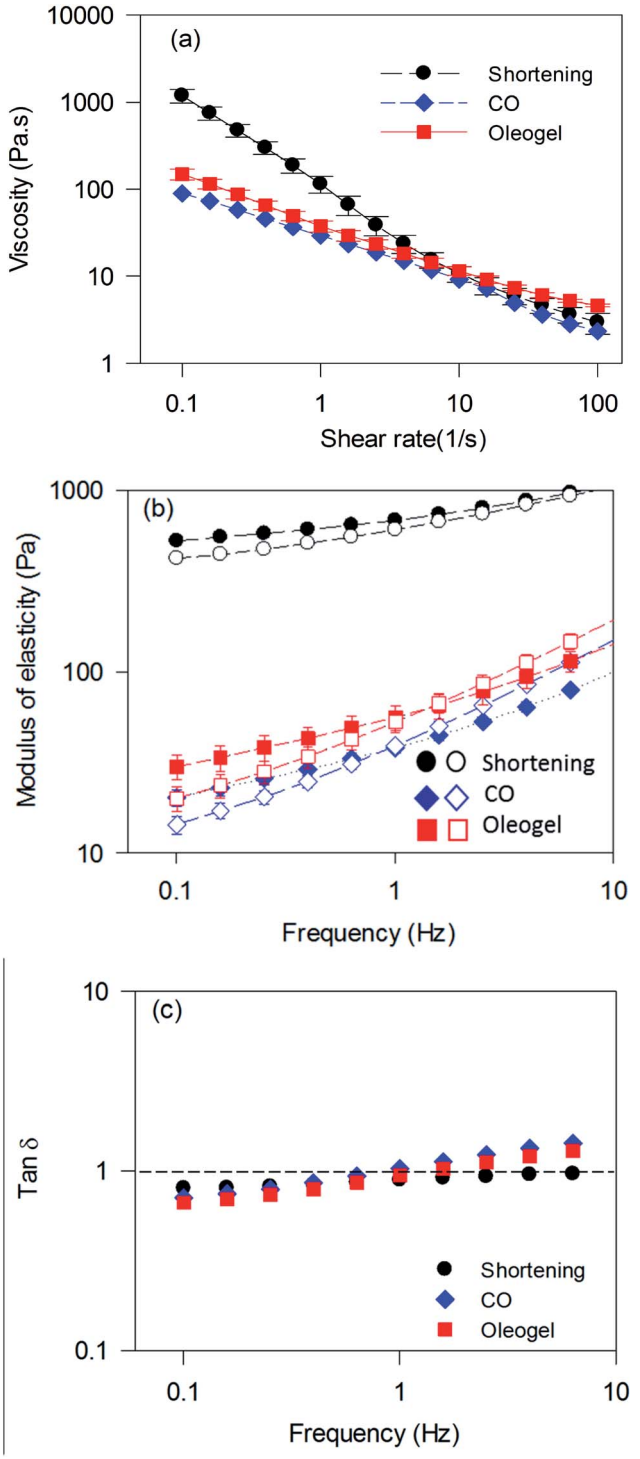

Fig. 8 Rheological properties of cake batters: (a) viscosities measured as a function of shear rate, (b) storage (G') and loss modulus (G''), and (c) tan δ of cake batters measured as a function of frequency at a constant strain of 0.05%. Dotted line in (c) is used to show tan $\delta = 1$.

oleogel batters (Fig. 7c and f) compared to shortening batter (Fig. 7a and d) is in the size, number and morphology of air bubbles, and protein–carbohydrate phase distribution. The air bubbles in the fat phase of CO and oleogel batters are much larger, fewer, which could be responsible for their higher specific gravity. The surfaces of the air bubbles were also distinctively irregular in the two former batters (Fig. 7e and f) compared to the shortening batter (Fig. 7d). The protein–carbohydrate mixed-phase was also discretely distributed in the fat phase of the CO and oleogel batters. A similar change in the microstructure of cake batter was also observed when solid fat was replaced with rapeseed oil,[33] which was ascribed to the poor gluten development in these batters.

Optimum batter rheology is required to incorporate air bubbles as well as to stabilize them during baking.[34] The change in batter viscosity with respect to the change in shear rate is displayed in Fig. 8a. All three batter samples showed pseudo-plastic behaviour, where viscosity decreased with an increase in shear rate. The batter prepared using shortening displayed about 6-times higher viscosity at a lower shear rate (less than 0.1 s^{-1}) compared to the batters prepared using the oleogel and CO (Fig. 8a). Reduction in viscosity and increase in specific gravity of batters were also reported when shortening was replaced by sesame oil[35] and rapeseed oil.[33]

Fig. 8b and c show the frequency-dependent viscoelastic properties of cake batters. All batters displayed higher G' than G'' in the lower frequency range, but both G' and G'' reduced significantly when shortening was replaced by CO or the oleogel. tan δ (ratio of G'' to G') for shortening batter increased with an increase in frequency but remained less than 1 throughout the frequency range, indicating dominant elastic behaviour. Both CO and oleogel batters briefly displayed lower tan δ than shortening batter below 0.5 Hz frequency; however, it raised rapidly going over more than 1 beyond 1 Hz, indicating transformation from elastic to viscous behaviour. The higher viscosity and gel strength of shortening batter compared to the others could be attributed to the presence of solid fat crystals and the associated stabilization of a higher amount of air. Similar changes in batter rheology were also observed when shortening was replaced with wax-based oleogel[3,17] and HPMC foam-stabilized oleogel[3] in the preparation of muffin batters. Although the oleogel consists of a significant amount of liquid oil, it's batter showed slightly higher G' than CO batters, which could be due to increased air incorporation and water-binding capacity of the pea proteins.[36] It has been reported that water-binding capacity of ingredients reduce availability of free water and movement of particles during shear leading to an increased viscosity.[37] A higher G' was also observed when HPMC foam-stabilized oleogels were utilized for batter preparation compared to a liquid oil, which was ascribed to the higher amount of air incorporation in the former.[6]

3.3.2. Evaluation of cakes made with oleogel and other fats. The images of the final cake products are shown in Fig. 9. Oleogel cakes displayed a more yellow colour than the others, which could be due to the pigments present in the PPC used for the oleogel preparation. The shortening cakes displayed a uniform distribution of small air bubbles and flour solids, while both CO and oleogel cakes displayed a non-uniform distribution of relatively large air bubbles in a dense network of cake matrix. Specific volumes of the cakes were determined to understand whether the change in fat could influence air incorporation (Table 1). Contrary to what has been reported in

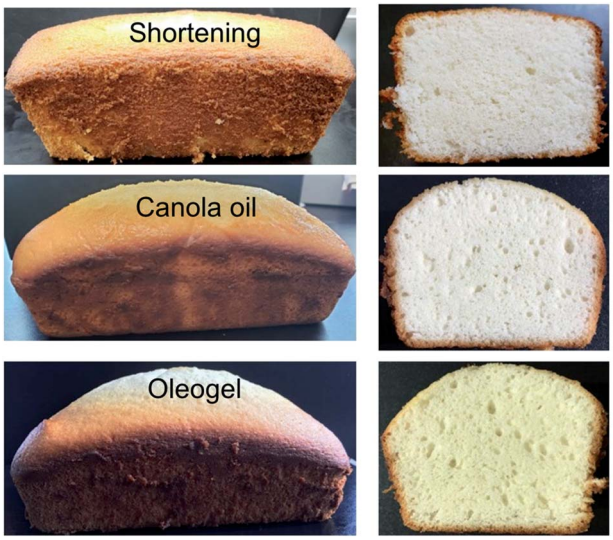

Fig. 9 The images of final cakes made with different types of fat. Cross section of the cakes is also shown on the right side.

the literature,[35] CO and oleogel cakes displayed similar specific volume ($p > 0.05$) as that of shortening cakes. These results indicate that batter microstructure and rheology at room temperature may not be used to predict the final cake volume, but the interaction of all ingredients and the change in their physicochemical properties during baking are also significant.

Texture profile analysis was performed on the cake samples to understand how the oleogel-based cakes would differ from traditional shortening-based cakes. An example of the texture profile curves for the three different cakes is shown in the ESI (Fig. S5†). The textural properties of different cakes (hardness, springiness, cohesiveness, chewiness), calculated from the "two-bite" texture profile analysis,[38] are compared in Fig. 10. Hardness, defined as the force necessary to attain a given deformation, was calculated from the height of the first peak (Fig. S5†).[38] Cohesiveness, a measure of internal bond-strength against 'chewing' action, was determined from the ratio of the second to the first peak area. The springiness of a cake is a measure of its compressibility during 'chewing', which was calculated from the length of the second compression to the total compression. Finally, chewiness, a secondary parameter, defined as the energy required to masticate a solid food product, was calculated from the product of primary parameters (hardness, cohesiveness and springiness).[17]

According to Fig. 10, oleogel cakes displayed higher hardness, springiness, and chewiness than the shortening cake ($p < 0.05$). The hardness and the chewiness of the oleogels cakes were double as that of the shortening cake. An increase in hardness and chewiness of cakes were also reported when shortening was replaced with foam-stabilized oleogels.[7] The cakes made with CO also displayed higher hardness and chewiness than the shortening cake, which were similar to the report of Sowmya *et al.*[35] Hardness is an indicator of staling of baked products. Monoglycerides present in the shortening

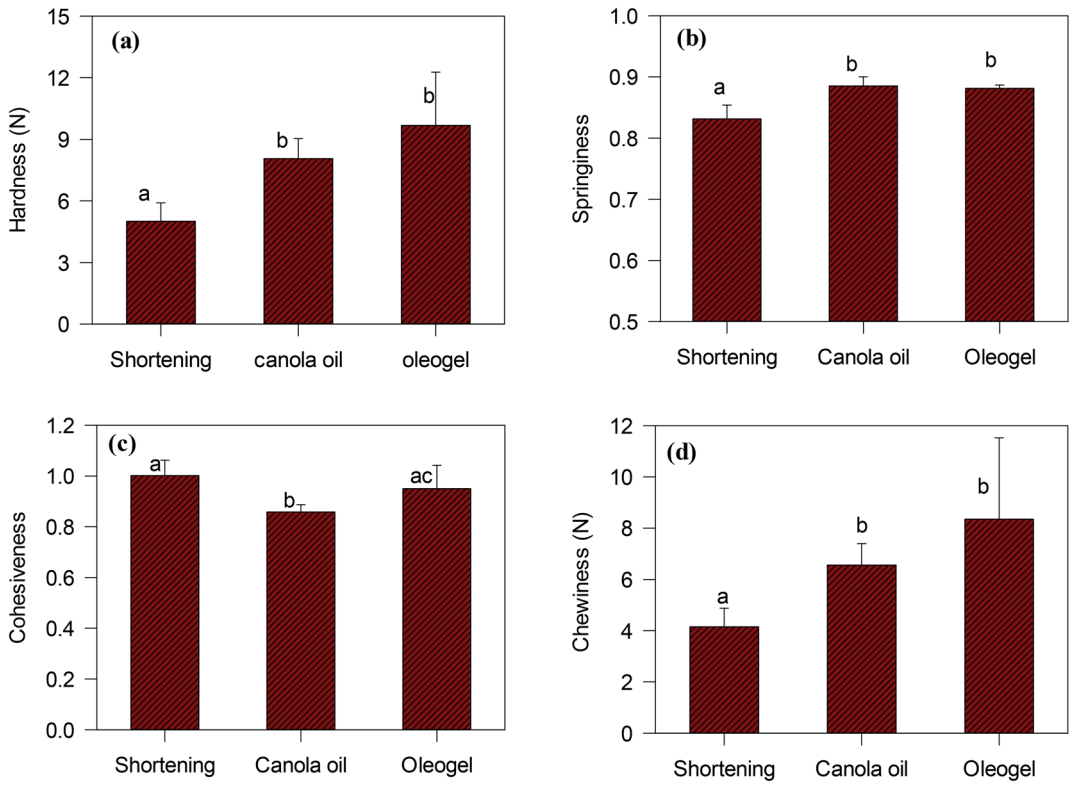

Fig. 10 Textural parameters (a) hardness, (b) springiness, (c) cohesiveness, and (d) chewiness of cakes prepared with different types of fat. Different letters in each graph indicate the difference between the values are statistically significant.

could form a complex with amylose of wheat flour and reduce the staling process,[39] which could produce a softer crust for the cake. Lack of monoglyceride might have facilitated adhesion of starch and protein particles[40] and resulted in higher hardness and chewiness of the CO and oleogel cakes.

Overall, the inability of the oleogel to stabilize the air bubbles during batter preparation and unwanted interaction between protein and starch remains a major issue limiting the quality of the cakes prepared with the oleogel. To overcome this, a small amount of solid fat, such as saturated monoglyceride or plant wax, might be added to the oil phase before adsorption into the foam matrix. It could improve oil binding capacities of the foam-stabilized oleogels and therefore texture and rheological properties of the oleogels. Moreover, emulsifiers such as saturated monoglyceride can help incorporate more air into the batter and develop a softer cake crust. In the future, we will incorporate them into the oleogels to improve the quality of the cakes.

4. Conclusions

Porous structures prepared by freeze-dried aqueous foams of PPC, PPI, FPC and FPI were found to bind liquid CO and lead to the formation of oleogels. Protein secondary structure uncovered using FTIR spectroscopy revealed that the freeze-dried foams interaction with oil changes protein conformation during oleogel preparation. Oil binding capacities of the foams were found to be controlled by the size, number and connectivity of the pores in the freeze-dried foams. The mechanical properties of the oleogels were influenced by the OBC, as well as the ability of the foams to retain oil under stress. The oleogels with higher oil content, made with foams stabilized by protein concentrates at pH 7 and pH 9, were less elastic and easily spreadable. Therefore, protein concentrates were better than the isolates for the preparation of oleogels using the foam-templated approach. In the end, cakes were successfully made using oleogel as a shortening alternative, but the textural qualities of the oleogel cakes were not as good as shortening cakes which could be ascribed to poor air incorporation in the oleogel batter and unwanted protein and starch interactions in the cakes, compared to the shortening.

Conflicts of interest

There are no conflicts to declare.

Acknowledgements

This work was supported by the Agriculture Development Fund (ADF) from the Saskatchewan Ministry of Agriculture, Canada – Saskatchewan Growing Forward 2 bi-lateral agreement, Saskatchewan Pulse Growers (project# 20160136); CFI-John R. Evans Leaders Fund (2012-31292), and Innovation and Science Fund (ISF) from Saskatchewan Ministry of Advanced Education.

References

1 A. R. Patel and K. Dewettinck, *Food Funct.*, 2016, **7**, 20–29.
2 M. Abdollahi, S. A. H. Goli and N. Soltanizadeh, *Eur. J. Lipid Sci. Technol.*, 2019, 1900196.
3 S. Lee, *Food Hydrocolloids*, 2018, **77**, 796–802.
4 L. Manzocco, F. Valoppi, S. Calligaris, F. Andreatta, S. Spilimbergo and M. C. Nicoli, *Food Hydrocolloids*, 2017, **71**, 68–75.
5 A. R. Patel, N. Cludts, M. D. B. Sintang, A. Lesaffer and K. Dewettinck, *Food Funct.*, 2014, **5**, 2833–2841.
6 A. R. Patel and K. Dewettinck, *Eur. J. Lipid Sci. Technol.*, 2015, **117**, 1772–1781.
7 A. R. Patel, D. Schatteman, A. Lesaffer and K. Dewettinck, *RSC Adv.*, 2013, **3**, 22900–22903.
8 A. De Vries, J. Hendriks, E. Van Der Linden and E. Scholten, *Langmuir*, 2015, **31**, 13850–13859.
9 A. De Vries, A. Wesseling, E. van der Linden and E. Scholten, *J. Colloid Interface Sci.*, 2017, **486**, 75–83.
10 S. Damodaran, *J. Food Sci.*, 2005, **70**, R54–R66.
11 A. Mohanan, M. T. Nickerson and S. Ghosh, *Accepted in Food Chemistry*, 2019.
12 H. Pehlivanoğlu, M. Demirci, O. S. Toker, N. Konar, S. Karasu and O. Sagdic, *Crit. Rev. Food Sci. Nutr.*, 2018, **58**, 1330–1341.
13 J. Kong and S. Yu, *Acta Biochim. Biophys. Sin.*, 2007, **39**, 549–559.
14 AACC International, *Approved Methods of Analysis, 11th edn, Method 90-10.01, Baking Quality of Cake Flour*, approved October 08, 1976, reapproval November 3, 1999, AACC International, St. Paul, MN, U.S.A., 1999.
15 AACC International, *Approved Methods of Analysis, 11th edn, AACC Method 10-05.01 Guidelines for Measurement of Volume by Rapeseed Displacement*, AACC International, St. Paul, MN, U.S.A., 2001.
16 J. Y. Kim, J. Lim, J. Lee, H. S. Hwang and S. Lee, *J. Food Sci.*, 2017, **82**, 445–452.
17 H. H. Friedman, J. E. Whitney and A. S. Szczesniak, *J. Food Sci.*, 1963, **28**, 390–396.
18 J. Pinto, A. Athanassiou and D. Fragouli, *J. Phys. D: Appl. Phys.*, 2016, **49**, 145601.
19 M. O. Adebajo, R. L. Frost, J. T. Kloprogge, O. Carmody and S. Kokot, *J. Porous Mater.*, 2003, **10**, 159–170.
20 S. Turgeon, C. Schmitt and C. Sanchez, *Curr. Opin. Colloid Interface Sci.*, 2007, **12**, 166–178.
21 K. Lomakina and K. Mikova, *Czech J. Food Sci.*, 2006, **24**, 110–118.
22 S. Damodaran, *Protein functionality in food systems*, 1994, pp. 1–37.
23 P. J. Hailing and P. Walstra, *Crit. Rev. Food Sci. Nutr.*, 1981, **15**, 155–203.
24 F. A. Husband, P. J. Wilde, A. R. Mackie and M. J. Garrood, *J. Colloid Interface Sci.*, 1997, **195**, 77–85.
25 H. Wu, Y. Fan, J. Sheng and S.-F. Sui, *Eur. Biophys. J.*, 1993, **22**, 201–205.
26 E. Dickinson, *Colloids Surf., B*, 1999, **15**, 161–176.
27 Z. Meng, K. Qi, Y. Guo, Y. Wang and Y. Liu, *Food Chem.*, 2018, **246**, 137–149.
28 F. R. Lupi, V. Greco, N. Baldino, B. de Cindio, P. Fischer and D. Gabriele, *J. Colloid Interface Sci.*, 2016, **483**, 154–164.

29 M. Suzuki, Y. Nakajima, M. Yumoto, M. Kimura, H. Shirai and K. Hanabusa, *Langmuir*, 2003, **19**, 8622–8624.
30 M. Ahmadi, A. Madadlou and A. A. Saboury, *Food Chem.*, 2016, **196**, 1016–1022.
31 E. Wilderjans, A. Luyts, K. Brijs and J. A. Delcour, *Trends Food Sci. Technol.*, 2013, **30**, 6–15.
32 J. Wootton, N. Howard, J. Martin, D. McOsker and J. Holme, *Cereal Chem.*, 1967, **44**, 333–343.
33 N. Hesso, C. Garnier, C. Loisel, S. Chevallier, B. Bouchet and A. Le-Bail, *Food Struct.*, 2015, **5**, 31–41.
34 F. Ronda, B. Oliete, M. Gómez, P. A. Caballero and V. Pando, *J. Food Eng.*, 2011, **102**, 272–277.
35 M. Sowmya, T. Jeyarani, R. Jyotsna and D. Indrani, *Food Hydrocolloids*, 2009, **23**, 1827–1836.
36 J. P. Peters, F. J. Vergeldt, R. M. Boom and A. J. van der Goot, *Food Hydrocolloids*, 2017, **65**, 144–156.
37 S. F. Dogan, S. Sahin and G. Sumnu, *Eur. Food Res. Technol.*, 2005, **220**, 502–508.
38 M. Peleg, *J. Food Sci.*, 1976, **41**, 721–722.
39 S. Cauvain, *Trends Food Sci. Technol.*, 1998, **9**, 56–61.
40 K. Mattil, *Bailey's industrial oil and fat products*, 1964, pp. 265–388.